Composite Cu-$LaFeO_3$ Conversion Coatings on a 18Cr Ferritic Stainless Steel for IT-SOFC Interconnects: Effect of Long-Term Air Exposure at 700°C on Cr Diffusion Barrier and Electrical Properties

S. Frangini,[1,*,z] A. Masi,[2] L. Della Seta,[1] M. Bianco,[3] and J. Van Herle[3]

[1]*DTE-PCU-SPCT, ENEA CR Casaccia, 00123 Rome, Italy*
[2]*Università Roma Tre, Dipartimento di Ingegneria, 00146 Rome, Italy*
[3]*GEM group, Inst. Mech. Eng., EPFL Valais, CH-1951 Sion, Switzerland*

In our previous study copper oxide additions were used to accelerate the formation of perovskite $LaFeO_3$ conversion coatings on stainless steels from molten carbonate baths. Incorporation of copper particles into the growing coating was an additional effect resulting in the formation of a composite Cu-$LaFeO_3$ structure. In continuation to our previous study, the aim of this work is to report the effect of copper additions on long-term stability and performance of perovskite conversion coatings under IT-SOFC interconnect conditions. To this end, a Cu-$LaFeO_3$ coated K41 18Cr ferritic stainless steel was examined in air at 700°C up to 1000 h. In order to simulate properly the situation of a real IT-SOFC cell, Area Specific Resistance (ASR) and Cr-barrier properties of the coated steel were evaluated simultaneously with a special coating characterization setup. Studies were conducted by comparison with single-phase $LaFeO_3$ coatings obtained in a molten carbonate bath similar to that used for the formation of the composite Cu-$LaFeO_3$ coatings but without the addition of copper oxide. Copper addition did not change the general morphology of the perovskite coating, which remains a multi-layer coating, being composed of an outer $LaFeO_3$ crystalline layer, a middle Fe-rich oxide and two inner Fe-Cr rich oxide layers. However, copper was beneficial in promoting a thinner and more stable coating structure along with finer perovskite grain size. These structural improvements were further confirmed by the results obtained with electrical measurements that showed a better ASR behavior of the Cu-$LaFeO_3$ coatings. On the other hand, no relevant copper effects could be detected on the coating oxidation stability and on the Cr-barrier properties of the perovskite conversion coatings. Both $LaFeO_3$ and Cu-$LaFeO_3$ coatings showed similarly high coating stability and excellent Cr-barrier capability in experiments conducted at 700°C up to 1000 h. In definitive, dual-phase Cu-$LaFeO_3$ seem more promising systems for IT-SOFC interconnects than single-phase $LaFeO_3$ conversion coatings, although further improvements in ASR electrical properties are needed.
 [DOI: 10.1149/2.0101803jes]

Manuscript submitted December 13, 2017; revised manuscript received January 26, 2018. Published February 6, 2018.

Conventional 18Cr ferritic stainless steels are promising candidates for Intermediate Temperature Solid Oxide Fuel Cell (IT-SOFC) interconnects as they provide an optimal combination of cost, structural and chemical composition properties.[1–3] However, the use of 18Cr ferritic stainless steels is not without its cost. Issues are related to formation of insulating chromia layers with high tendency to evaporate during their exposure to the IT-SOFC operating conditions. Hence, coating with a ceramic layer made of electro-conductive and corrosion-resistant spinel[4] or perovskite[5] oxides is usually considered a necessary addition for ensuring a stable and low Area Specific Resistance (ASR), which is a common way to express interfacial ohmic resistance in electrochemical devices. In particular, (Co-Mn) or (Cu-Mn)- based spinel oxides as well as (La-Cr), (La-Co) or (La-Mn) perovskite oxides have shown also great potential as Cr diffusion barrier for suppressing the degradation cell performance caused by Cr contamination of the cathode layer, which could occur as a result of Cr evaporation and diffusion from the steel interconnects.[2,6] For more definitive results, coatings with improved properties and industrially scalable coating technologies at acceptable costs are still an active area of current IT-SOFC materials research. In this context, development of a novel perovskite conversion coating process has been the subject of our recent studies in an attempt to develop alternative coating strategies for the corrosion protection of ferritic stainless steel IT-SOFC interconnects.[7–12]

In short, the process enables the formation of a continuous, dense and adherent multi-layer coating consisting of an outer $LaFeO_3$ perovskite layer and precursor iron-rich oxide sub-layers. The perovskite layer forms by selective reaction of the steel iron component with a lanthanum oxide reactant dissolved in an oxide ion-buffered molten carbonate bath, at ca. 600°C. As opposed to iron, under the oxide-buffered melt conditions, the common steel alloying elements such as chromium and nickel form soluble oxide-ion containing complexes rather than solid products, being thus selectively removed for the near-surface of the steel and confined in the sub-coating regions of the steel. By adjusting the acid-base chemistry of the carbonate melt, it is possible to produce thin- or thick-film conversion coatings with thicknesses variable from a few microns to up to ca. 20–25 microns and with different electrical and Cr diffusion barrier properties.[8,10,12]

Our latest studies on thick-film perovskite coatings have indicated that the conversion process can be significantly accelerated by addition of copper oxide in the molten carbonate bath. During the process, copper particles are also incorporated in the growing coating resulting in the formation of a composite metal-perovskite structure.[11] Formation mechanism and coating microstructure have been investigated in detail focusing on Cu-$LaFeO_3$ coatings grown on a commercial 18Cr ferritic stainless steel. The study has shown that deposition of the copper metallic particles occurred by a galvanic displacement mechanism, by which copper reduction is coupled to iron oxidation.[11] Preliminary coating stability studies at 700°C have indicated that the composite metal-perovskite layer is a stable and effective barrier for outward Cr diffusion, at least during a short-term 200 h exposure.

In continuation of our previous work, the aim of this study is therefore devoted to investigate in more detail the effect of copper on long-term stability and performance of $LaFeO_3$ perovskite coatings under IT-SOFC interconnect conditions. To this end, electrical, chemical and barrier diffusion properties of a coated K41/441 grade 18Cr ferritic stainless steel has been investigated at 700°C by using a special coating characterization setup. The experiments have been carried out by comparing composite Cu-$LaFeO_3$ with structurally-similar Cu-free $LaFeO_3$ perovskite conversion coatings.

*Electrochemical Society Member.
[z]E-mail: stefano.frangini@enea.it

Experimental

A 0.2 mm-thick plate of commercial K41 ferritic 18Cr stainless steel with a nominal composition of (Fe-17.7Cr-0.6Si-0.65(Ti+Nb)-0.3Mn-0.015C, in wt%) was used as substrate steel in this work. Squared foils of 40 × 40 mm size were cut from the plate and then used for the coating treatment. The foils were mechanically polished up to 1200 grit finish, ultrasonically cleaned in acetone and dried prior to applying the iron chemical conversion coating treatment.

Preparation of thick-film composite Cu-$LaFeO_3$ coated K41steel was performed under optimal synthesis conditions as individuated in our previous work.[11] The coating treatment was carried out by deeply immersing the steel samples in a binary $(LiNa)_2CO_3$ eutectic molten carbonate bath containing the following additives: La_2O_3 (1 mol %), MgO (3 mol%) and CuO (4 mol %). The molten carbonate treatment was conducted at 600°C for 24 h under a CO_2 gas bubbling condition. These samples will be identified as Cu-$LaFeO_3$ coatings in the following.

For comparison purposes, a molten carbonate bath of similar composition but not containing copper oxide accelerants was used to prepare single-phase $LaFeO_3$ perovskite conversion coatings. In this case, the binary $(LiNa)_2CO_3$ eutectic molten carbonate bath contained the following additives: La_2O_3 (1 mol %) and MgO (10 mol %). The coating treatment was carried out at the same temperature and CO_2 gas bubbling as used for the composite coating synthesis. However, owing to the absence of copper oxide accelerants, a longer duration of the treatment (48 h) was required for a complete surface coverage by the conversion coating as reported in our previous studies.[8] These samples will be identified as $LaFeO_3$ coatings in the following.

The coated samples were subjected to oxidation experiments carried out in laboratory air at 700°C on alumina plates, to evaluate the coating stability by means of morphological (SEM/EDX) and structural (XRD) analysis. After 200 h of treatment, the coupons were characterized. Some of the exposed samples were rinsed in distilled water and exposed further up to 1000 h.

ASR and Cr-barrier properties of the coatings were measured simultaneously through a novel testing system specifically developed in the framework of the EU Scored 2.0 project, whose details can be found in Ref. 13. Briefly, the testing system consists of a multi-sample stack with the samples electrically connected in series and arranged to form a sandwich structure. L-shaped coated steel samples with an active area of 1 cm^2 were laser cut and each lamella sample was put in contact with a symmetrical Pd L-shaped lamella. Notably, the touching side of the Pd lamella is covered with 20 μm, Lanthanum Strontium Cobaltite (LSC) perovskite cathode material. The steel/perovskite/LSC/Pd interface is meant to replicate the SOFC cell stack cathode contact condition. Repetitions of this unit contact cell creates the overall tested samples sandwich. An uniform pressure contact of 0.4 MPa to the whole sandwich cell is ensured by proper metallic clamping systems. A four-probe method is applied for continuous measurement of the ASR under a constant current of 0.4 Acm^{-2} flowing through the stack. The resistance is measured as ratio between the voltage drop occurring in a single contact cell unit (ΔV) and the constant current load. The voltage drop is measured by two leading wires welded onto the small tongue terminals of the L-shaped coated steel and Pd plates, and connecting them to an Agilent Data Acquisition unit (Mod. 34970a).

Figure 1 describes the stack test apparatus showing a multi-sample stack with four contact cell units. The stack is inserted in a chamber furnace, heated up to 700°C and kept at this temperature for 1000 h under a 1 NL/min flowing 3%vol. H_2O- air atmosphere. As clearly seen in Figure 1, each contact cell unit consists of multiple resistive contributions to the measured voltage drop across the Pd plate and the coated steel sample. Hence, the ASR is derived from the measured voltage drop with the assumption that the contribution to the ohmic losses at the steel/coating interface is at least one order of magnitude higher than at the other contact interfaces and through the LSC paste. For instance, at 700°C, the electrical resistivity of chromia lies in the range 10–10^3 Ωcm,[14] which is several orders of magnitude higher than

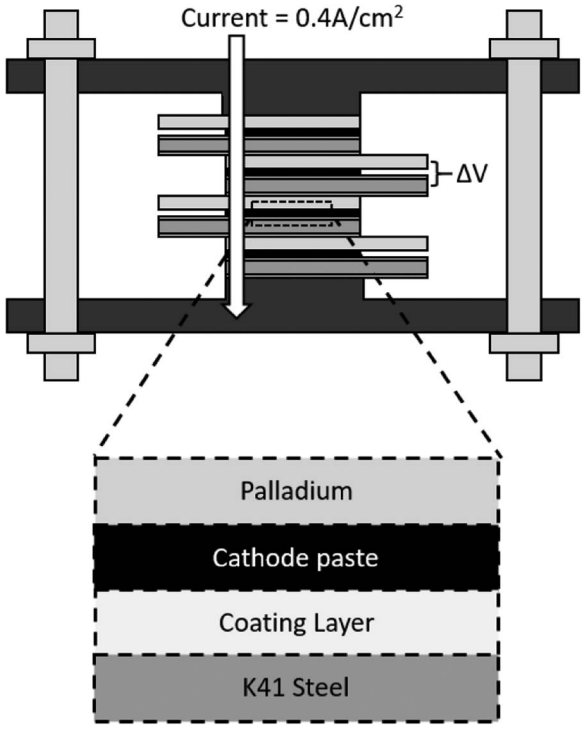

Figure 1. Schematic representation of the ASR/Cr diffusion experimental setup.

that reported for the LSC cathode.[15] Besides, the method has been previously validated with a commercial Ce/Co coated Sandvik Sanergy HT steel used as benchmark:[13] a very low contact cell unit resistance (ca. 5 $m\Omega cm^{-2}$) has been measured at 700°C, in perfect agreement with ASR literature data.[16] Therefore, it follows that resistance of each single contact cell unit (R_{cell}) can be reasonably approximated to the ASR of the LSC/steel interface as follows:

$$\frac{\Delta V_{measured}}{I} = R_{cell} \cong ASR_{coating}$$

Since appreciable amounts of salt residues containing cation contaminants such as Cr may remain attached to the coated surfaces, a cleaning up step was adopted to prevent spurious results in the subsequent ASR/Cr diffusion tests. Our previous studies demonstrated that washing in boiling deionized water for 6 h is successful in most cases, particularly with easy-to-clean, smooth coated surfaces.[9,10] Nevertheless, additional more drastic clean-up treatments may be required for full removing residual carbonate salt from more geometrically-complex coating surfaces due to carbonate salt tendency to strongly adhere on metallic surfaces.[17] Hence, a batch of coated steel samples was subjected to an additional oxidation treatment in moist air at 700°C for 200 h to accelerate evaporation of any strong-adherent surface salt residue. In the following, these pre-oxidized steel samples will be identified as "$LaFeO_3$ pre-ox" and "Cu-$LaFeO_3$ pre-ox" samples. Post-test analysis was used to evaluate Cr diffusion barrier properties of the coated steel samples. Hence, after the completion of the ASR test, the stack was removed from the furnace, embedded in epoxy resin, cut and polished.

Microstructure and chemical composition analysis were performed using a JEOL JSM-5510LV Scanning Electron Microscope (SEM) equipped with an Energy-dispersive X-ray microanalysis (EDX). X-Ray Diffraction (XRD) analyses were carried out with a Seifert PAD VI diffractometer, equipped with a Mo Kα radiation source and a LiF monochromator on the diffracted beam.

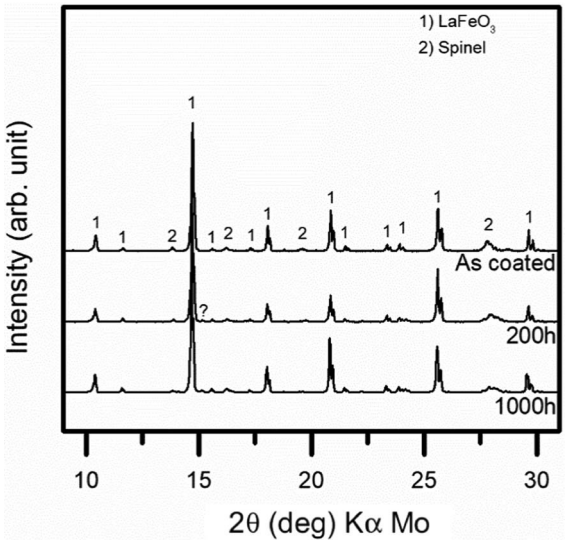

Figure 2. XRD patterns of $LaFeO_3$ coated steel samples after the coating treatment and after 200 h and 1000 h of oxidation in air at 700°C.

Results and Discussion

Coating stability studies.—XRD patterns of the $LaFeO_3$ samples before and after 200 h and 1000 h treatment in air at 700°C are reported in Figure 2. All patterns are characterized by similar features, with main peaks ascribable to a $LaFeO_3$ perovskite phase and minor peaks ascribable to a Fe-rich spinel phase. Peak position of the spinel phase is compatible with several Fe-rich spinel phases, such as magnetite (Fe_3O_4), lithiated magnetite ($LiFe_5O_8$) or chromium-iron spinels ($FeCr_2O_4$), giving a pattern similar to that earlier observed in Cu-LaFeO3 coatings.[11] No significant changes are visible after the high temperature exposure, suggesting high stability of the crystalline phases. A subtle peak at 2θ∼15° is also observed in the 200 h treated sample. This peak may be due to the presence of mixed Fe-Cr (III) oxides, but is not unambiguously assignable.

SEM images of the $LaFeO_3$ samples is reported in Figure 3. The as-coated sample surface, depicted in Figure 3a, is characterized by the presence of large perovskite crystallites with a wide size distribution range around an average value of ca. 10 μm. The oxidation treatment induces a smoothening of the crystals edges, yet without significantly affecting coating morphology and crystallite sizes. A complete characterization of the $LaFeO_3$ crystallite size distribution in terms of mean, standard deviation, median and mode parameters was obtained by manually determining particle diameter for 100 crystallites using SEM images. The results, given in Table I, indicate a symmetric distribution of crystallite sizes. The section of the $LaFeO_3$ samples is depicted in Figure 4 and the results of EDX analysis collected on the spots reported in the figure is summarized in Table II. Starting from the as coated specimen (Figure 4a, several distinct layers can be observed. Analyzing EDX results, it is evident the presence of the perovskite (point 1) on the outer surface, grown on a Fe-rich oxide (point 2). Underneath it, a 10 μm-thick Fe-Cr rich layer (point 3) followed by a well-distinct 2 μm-thick Fe-Cr rich interfacial scale (point 4) are formed on the steel substrate (point 5). A moderate growth of the Fe-Cr rich interfacial scale up to 4 μm is observed on the coated sample after exposure for 200 h, although no further scale growth could be observed between 200 and 1000h exposure (see Figures 4b and 4c). Other significant differences were not observed in the coating structure between 200 and 1000 h exposure except for a slight Mn enrichment of the Fe-Cr rich oxides (points 3 and 4). The overall coating thickness is about 25 um.

Table I. Statistical size distribution of perovskite crystallites grown on $LaFeO_3$ and Cu-$LaFeO_3$ coatings. Sizes are given in μm.

Parameter	$LaFeO_3$	Cu-$LaFeO_3$
mean	10	4
Standard deviation	±4	±1
Median	10	3
Mode	10	3

Regarding the Cu-$LaFeO_3$ samples, XRD patterns of the as coated and exposed samples are reported in Figure 5. Starting from the pristine sample, main peaks are ascribable to a $LaFeO_3$ perovskite phase, with minor reflections ascribable to metallic copper, to a partially reduced lithiated spinel phase ($Li_5Fe_5O_8$ – JCPDS card N. 40–943) and to substrate. After 200 h exposure in air at 700°C, the partially reduced Fe-rich spinel phase was completely reoxidized to a spinel phase similarly to that observed in the $LaFeO_3$ samples. Furthermore, very subtle peaks ascribable to a La-rich silicate ($LiLaSi_8$ – JCPDS card N. 48-6) appear, suggesting formation of a crystalline structure during the oxidation treatment, although these peaks were no longer clearly observable after 1000 h oxidation treatment.

SEM image of Cu-$LaFeO_3$ samples surface is reported in Figure 6. The as coated sample surface is covered by sharp-edged cubic perovskite crystallytes of about 4 μm average size, which

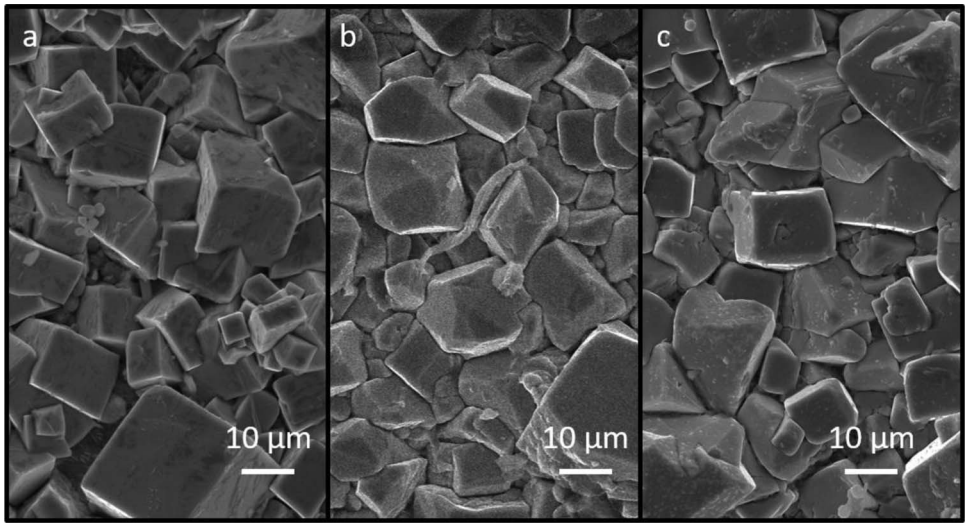

Figure 3. SEM images of $LaFeO_3$ coated steel samples surface after the coating treatment (a), after 200 h (b) and 1000 h (c) of oxidation in air at 700°C.

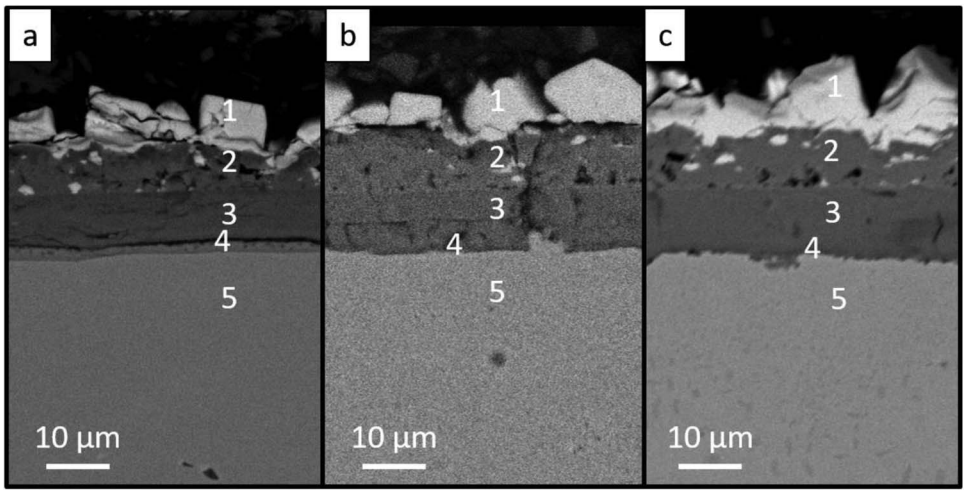

Figure 4. SEM images of $LaFeO_3$ coated steel samples section after the coating treatment (a), after 200 h (b) and 1000 h (c) of oxidation in air at 700°C, with superimposed EDX spot positions used for the chemical analysis (Table II). Positions correspond to different phase layers: 1. $LaFeO_3$; 2. Fe-rich oxide; 3. Fe-Cr oxide; 4. Fe-Cr oxide; 5. Steel matrix.

indicates that Cu addition to the salt bath promoted a substantial reduction in terms of mean and variability of the crystallite sizes as clearly seen from Table I. Moreover, conversely to the Cu-free $LaFeO_3$ coating, in this case the results shows a tail in the crystallite size distribution, possibly suggesting a change in the rate and mechanism of the crystallite formation process (see, for instance,[17]), although this aspect will be not further discussed being well outside the purpose of this work. Small rounded copper particles not evenly distributed are observable encased in the perovskite crystallytes. After being exposed to 200 h in air at 700°C, the perovskite morphology appears similar to the pristine coating, while small fibrous particles, rich in silicon and in lanthanum by EDX results, are observable. These fibers should correspond to the Lanthanum silicate phase peaks observed in the XRD patterns since the presence of the fiber crystallites is significantly reduced after 1000 h treatment, which is in accordance with the XRD results for this silicate phase. It is possible that the silicate phase was removed during the clean-up procedure of the samples after the 200 h treatment and before the further treatment up to 1000 h.

Table II. Elemental composition (wt%) as obtained by EDX analysis of $LaFeO_3$ samples section spots reported in Figure 4.

As coated

		Cation %			
Element	Point 1	Point 2	Point 3	Point 4	Point 5
Cr		0.8	43.6	36.6	18.6
Mn			0.5	0.8	0.5
Fe	39.0	98.9	55.7	62.4	80.8
La	61.0	0.2	0.2	0.1	

200 h oxidation

		Cation %			
Element	Point 1	Point 2	Point 3	Point 4	Point 5
Cr		0.9	47.3	50.0	12.5
Mn		0.1	0.5	1.9	
Fe	39.2	98.3	52.0	47.9	87.5
La	60.8	0.7	0.1	0.2	0.1

1000 h oxidation

		Cation %			
Element	Point 1	Point 2	Point 3	Point 4	Point 5
Cr		0.9	48.4	52.6	18.5
Mn			1.4	1.3	0.1
Fe	36.8	98.2	50.0	46.1	81.2
La	63.2	0.9	0.3		0.2

The presence of silicate phases on the coating surface requires some explanation. Since silicates are quite soluble in molten carbonates,[18] liquid extraction of silicon from the steel matrix is possible, which could explain the presence of silicate phases on the coating surface. In this sense, the presence of silicates on the surface of molten carbonate conversion layers was already observed in our previous studies.[10,12] Furthermore, a recent study can be used in support to our observations. This study indicates that carbonate melts can be used as efficient media for the synthesis of lithium-containing silicates but only when appropriate gas atmosphere conditions are used.[19] These findings suggest that acid-base salt conditions are crucial for silicate solubility and precipitation in molten carbonates. Thus, absence of silicate particles in the $LaFeO_3$ samples may indicate that coating synthesis occurred under acid-base salt conditions unfavourable for silicate precipitation.

The cross-section of Cu-$LaFeO_3$ samples is reported in Figure 7 showing also the EDX analysis points. The EDX results are reported in Table III. As already observed in our previous work,[11] the coating is characterized by a multi-layer structure, similar to the $LaFeO_3$ coated samples with the perovskite layer grown on a Fe-rich oxide

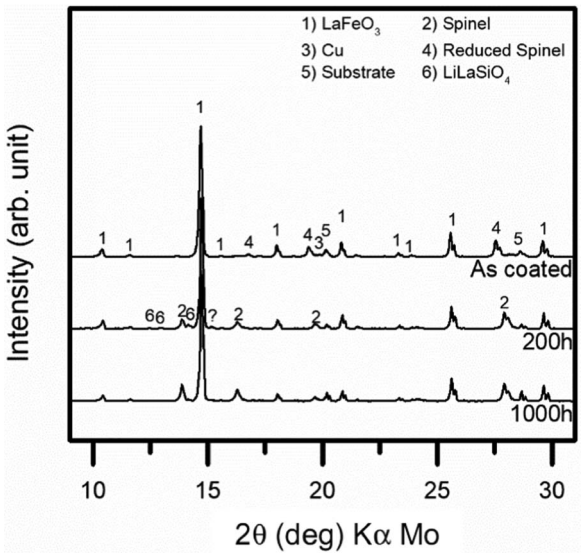

Figure 5. XRD patterns of Cu-$LaFeO_3$ coated steel samples after the coating treatment and after 200 h and 1000 h of oxidation in air at 700°C.

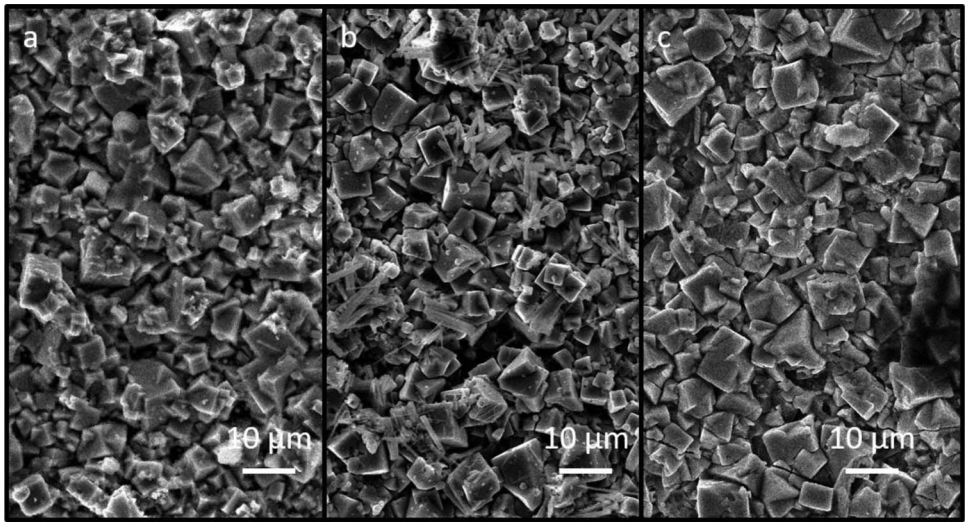

Figure 6. SEM images of Cu-$LaFeO_3$ coated steel samples surface after the coating treatment (a), after 200 h (b) and 1000 h (c) of oxidation in air at 700°C.

layer followed by a 5 µm-thick Fe-Cr oxide layer and a very thin Fe-Cr oxide interfacial scale with the steel. The Fe-Cr rich interfacial scale is significantly thinner (about 1 µm) as compared to the Cu-free $LaFeO_3$ coating. After the 200 and 1000 h oxidation treatment the thickness of the two inner layers of Fe-Cr rich oxide remains practically constant showing any measurable tendency to grow. In general, the coating structure as whole appears very stable, apart from a slight enrichment in manganese in the most interior oxide layers. A small, but significant presence of copper is detected mainly in the Fe-rich oxide layer after 1000 h treatment (see EDX point 2 of Figure 7c). This seems to confirm our previous results showing that some Cu inward diffusion could take place through the coating layer during high temperature treatment at 700°C possibly resulting in some improvement of coating electrical conductivity.[11] Furthermore, we have previously demonstrated that copper is useful as special additive for accelerating the coating conversion process. This work allows to highlight another important effect of copper addition. By direct comparison with the Cu-free $LaFeO_3$ coating samples it is clearly evident that copper addition affects not only the kinetics of the coating process, but also the coating morphology. With copper addition to the molten carbonate bath, in fact, perovskite crystallite size and overall coating thickness are both reduced to about half with respect to the Cu-free $LaFeO_3$ coating samples. This can have important implications for the functional properties of the perovskite conversion coatings, as it will be shown in the next section.

Some very preliminary studies on Cu-$LaFeO_3$ coating stability after a short-term oxidation treatment for 200 h were conducted in our previous work. A slight chromium-depleted zone of a few micron thickness was observed in the steel matrix at the metal/oxide interface.[11] In this work, the matrix Cr-depletion has been studied in more details. EDX analysis confirmed presence of Cr-depleted metal layers below the perovskite coating structure (see Table III, and in particular Cr content in Point 5 in the $LaFeO_3$ 200 h sample and in Point 5 in the Cu-$LaFeO_3$ 200 h and 1000 h sample). For a better understanding of the Cr-depletion phenomenon, the depth profile of the Cr/Fe ratio weight concentration within the entire steel matrix was estimated as a function of the oxidation treatment time. The results are reported in Figure 8. Prolonged oxidation treatment did not cause any significant change in the Cr/Fe ratio profile on both $LaFeO_3$ and Cu-$LaFeO_3$ coated samples. This indicates that the Cr-depletion layer does not extend deeper in the steel matrix, but remains limited to a few micron thickness even in the long-term period. The Cr-depleted zone is associated with Fe-Cr rich thin oxide layer grown at the coating/metal interface. The fact that the Cr-depleted zone does not gradually expand

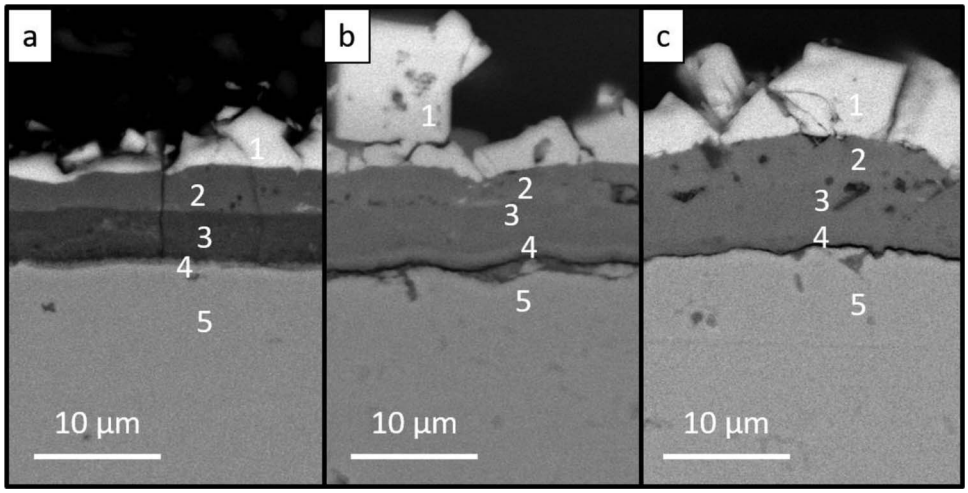

Figure 7. SEM images of Cu-$LaFeO_3$ coated steel samples section after the coating treatment (a), after 200 h (b) and 1000 h (c) of oxidation in air at 700°C, with superimposed EDX spot positions used for the chemical analysis (Table III). Positions correspond to different phase layers: 1. $LaFeO_3$; 2. Fe-rich oxide; 3. Fe-Cr oxide; 4. Fe-Cr oxide; 5. Steel matrix.

Table III. Elemental composition (wt%) as obtained by EDX analysis of Cu-$LaFeO_3$ samples section spots reported in Figure 7.

As coated

Cation %

Element	Point 1	Point 2	Point 3	Point 4	Point 5
Cr		1.8	51.4	44.5	18.9
Mn			0.6	0.6	0.3
Fe	40.4	97.5	47.1	54.7	80.7
Cu					
La	59.6	0.7	0.9	0.2	0.1

200 h oxidation

Cation %

Element	Point 1	Point 2	Point 3	Point 4	Point 5
Cr		8.0	53.1	68.9	16.8
Mn			0.7	2.7	0.3
Fe	39.5	90.6	45.3	28.2	82.8
Cu	0.3	0.7	0.2		
La	60.3	0.7	0.7	0.2	0.1

1000 h oxidation

Cation %

Element	Point 1	Point 2	Point 3	Point 4	Point 5
Cr		4.7	31.2	48.5	15.4
Mn			0.8	2.8	
Fe	39.0	92.6	67.9	48.8	84.6
Cu		2.8			
La	61.0				

means also that the Fe-Cr rich oxide layer is stable and its thickness does not increase with the time.

ASR electrical behavior.—Figure 9 shows the ASR behavior of the coated K41 steel samples during 1000 h of exposure at 700°C. The first 50 h data sets have been omitted to eliminate initial random fluctuations observed in the data. In general, composite Cu-$LaFeO_3$ coated samples show lower ASR in comparison to the LaFeO3 coatings, although all the ASR values remain relatively high (above 100 $m\Omega cm^{-2}$) and are not stabilized even after 1000 h of exposure. A maximum spread of data is observed between the non pre-oxidized samples with a minimum value of 110 $m\Omega cm^{-2}$ for the Cu-$LaFeO_3$ and a maximum of 230 $m\Omega cm^{-2}$ for the $LaFeO_3$ coated sample, after 1000 h of exposure. Conversely, the pre-oxidation treatment has the effect of reducing considerably the ASR differences to just a few $m\Omega cm^{-2}$. The better electrical properties of the Cu-$LaFeO_3$ sample can be attributed to an improved coating morphology with respect to the $LaFeO_3$ sample, although a coating morphology effect is not obvious in the pre-oxidized coated samples.

The ASR evolution shows a common decreasing trend for all the samples from 300 h of exposure onwards, with a tendency to a gradual linearization of the curves over the time. A similar downward trend in ASR has been sometimes reported in literature, but not commonly and possibly attributed to changes in electrical conductivity, densification or reaction sintering of the deposited coatings during the testing.[20,21] The rate of ASR change has been estimated in the linear portion of the curves. The rate of ASR decrease is more than twice for the Cu-LaFeO3 coatings (ca. 6 vs 2–3 $m\Omega cm^{-2}$ /100 h) and it is essentially independent on the pre-oxidation treatment. These results seem to confirm that coating morphology of the Cu-$LaFeO_3$ sample is an important factor with positive consequences on the electrical properties of the perovskite conversion coatings. In particular, SEM analysis has shown that Cu addition distinctly promotes a structural coating improvements in terms of a reduced overall coating thickness and also a reduced size of the perovskite crystallites. The formation of a very thin and stable Fe-Cr interfacial layer is an additional structural improvement induced by Cu additions to the bath, which could explain, at least in part, the improved ASR behavior of Cu-$LaFeO_3$ as compared to the Cu-free $LaFeO_3$ coatings.

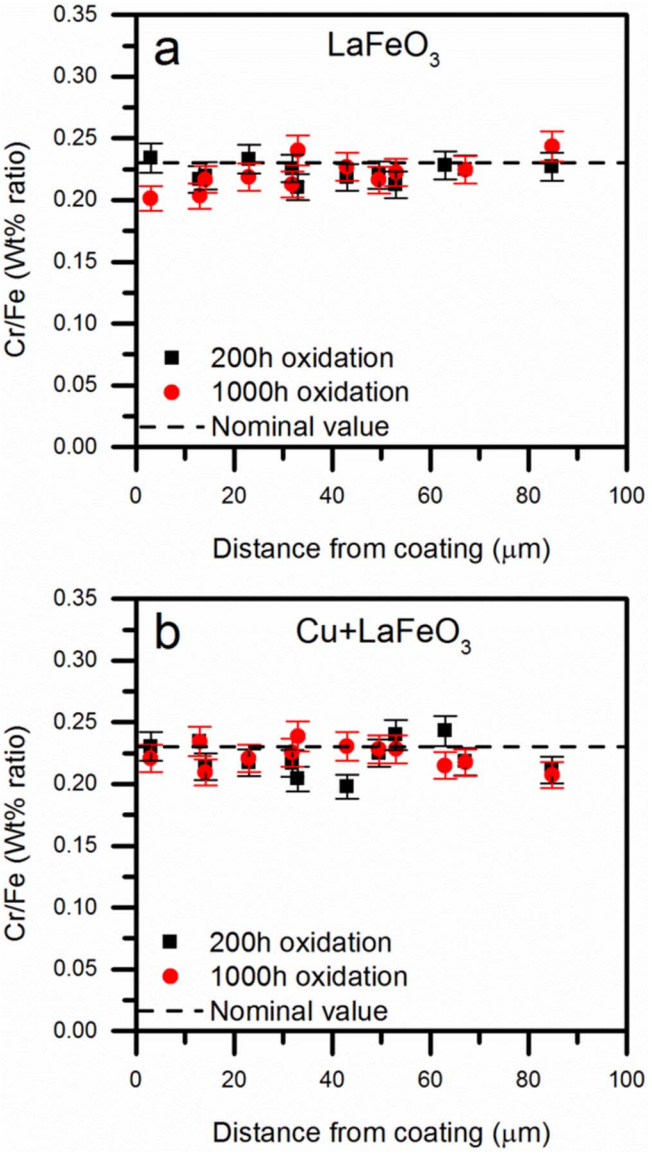

Figure 8. Results of the in depth profile analysis of the Cr/Fe ratio: (a) $LaFeO_3$ coated steel and (b) Cu-$LaFeO_3$ coated steel sample.

During the metallographic preparation of the samples, it was noted some detachment of the contact interface between the coated steel sample and the LSC cathode paste. This could signify that a proper electrical contact was not ensured during the test probably due to the excessive roughness of the perovskite coating that prevented a good contact with the LSC cathode layer. However, one can assume that a weak contact interface is not stable over time under the present experimental conditions. A tendency to a more compliant interface during the ASR test can be envisaged due to mechanical effects induced by the applied pressure. Thus, the observed downward trend in ASR could be at least in part due to an increasing contact area during the test. This also suggests that the actual ASR values should be lower than those experimentally determined.

Post-test analysis.—Cross section SEM analysis of the $LaFeO_3$ samples subjected to the ASR/Cr retention test are reported in Figures 10a and 10b, respectively for the as-coated samples and for the $LaFeO_3$ pre-ox samples. The Pd plate with the LSC cathode paste can be observed at the top of the image, with the steel at the bottom. As already mentioned in the previous section, large parts of the coating interface are not in contact with the LSC paste. Although the

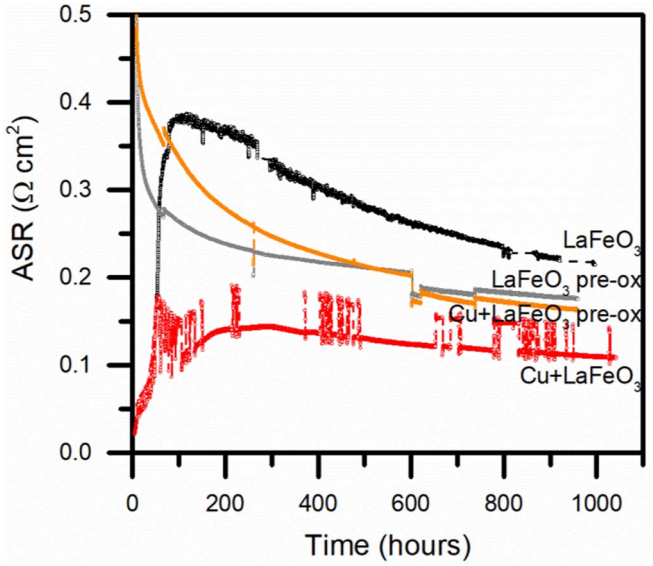

Figure 9. ASR values measured for the different samples as a function of the exposure time.

detachment could be somewhat exacerbated by the metallographic preparation, the high coating roughness seems to be the most likely cause preventing a good contact surface area.

Regarding the coating morphology and chemical composition, there is no particular difference with respect to the structure observed in the coating stability experiments, as further suggested by the EDX results in Table IV. No significant differences can be observed between the as-coated and the pre-oxidized samples after the ASR/Cr retention testing.

Figure 11 depicts the cross-section SEM analysis of Cu-$LaFeO_3$ subjected to the ASR/Cr retention test with the corresponding EDX results reported in Table V. The rough crystal morphology suggests a poor electrical contact with the LSC layer even in this case. Regarding the coating structure, no significant differences are observed with respect the coating stability studies and among the as-coated and the

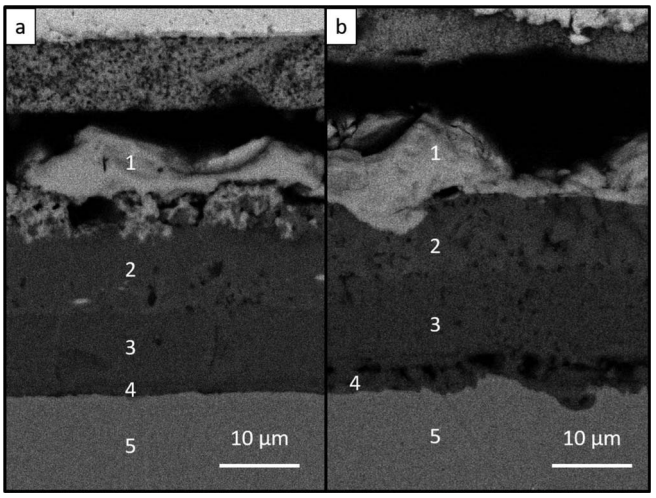

Figure 10. SEM images of $LaFeO_3$ coated steel samples section after 1000 h of exposure at 700°C in the ASR/Cr retention measurement setup: a) exposed as coated; b) exposed after 200 h of pre-oxidation in air at 700°C (see text for details). Numbers indicate the EDX spot positions for the chemical analysis results reported in Table IV. Positions correspond to different phase layers: 1. $LaFeO_3$; 2. Fe-rich oxide; 3. Fe-Cr oxide; 4. Fe-Cr oxide; 5. Steel matrix.

Table IV. Elemental composition (wt%) as obtained by EDX analysis of $LaFeO_3$ samples section spots reported in Figure 10.

LaFeO3

Cation %

Element	Point 1	Point 2	Point 3	Point 4	Point 5
Cr		0.4	60.5	62.9	16.9
Mn			2.0	2.4	
Fe	39.3	99.3	38.5	34.7	83.1
La	60.7	0.3			

LaFeO3 pre-ox

Cation %

Element	Point 1	Point 2	Point 3	Point 4	Point 5
Cr		1.4	53.1	72.2	14.6
Mn			1.4	1.4	
Fe	41.0	98.6	45.5	26.4	85.4
La	59.0				

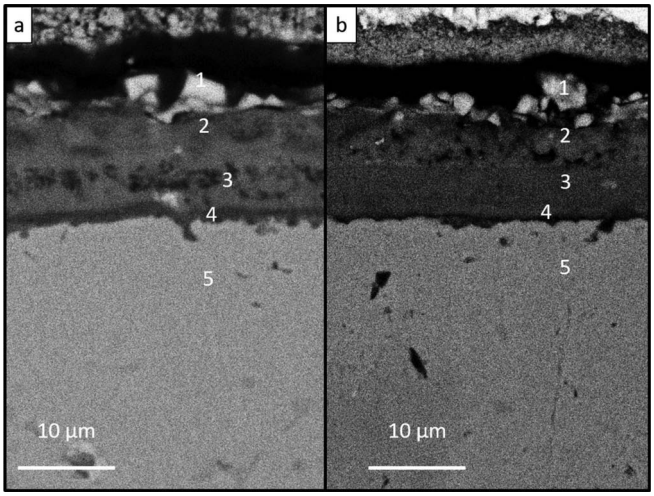

Figure 11. SEM images of Cu-$LaFeO_3$ coated steel samples section after 1000 h of exposure at 700°C in the ASR/Cr retention measurement setup: a) exposed as coated; b) exposed after 200 h of pre-oxidation in air at 700°C (see text for details). Numbers indicate the EDX spot positions for the chemical analysis results reported in Table V. Positions correspond to different phase layers: 1. $LaFeO_3$; 2. Fe-rich oxide; 3. Fe-Cr oxide; 4. Fe-Cr oxide; 5. Steel matrix.

Table V. Elemental composition (wt%) as obtained by EDX analysis of Cu-$LaFeO_3$ samples section spots reported in Figure 11.

Cu-LaFeO3

Cation %

Element	Point 1	Point 2	Point 3	Point 4	Point 5
Cr		1.4	56.1	82.8	17.6
Mn			1.3	2.1	
Cu	1.4	1.3			
Fe	37.9	96.8	42.5	14.4	82.4
La	60.6	0.5		0.7	

Cu-LaFeO3 pre-ox

Cation %

Element	Point 1	Point 2	Point 3	Point 4	Point 5
Cr		1.2	53.5	43.8	18.9
Mn			4.1	5.5	
Cu	1.9	1.2	1.3		
Fe	40.1	97.6	40.6	50.8	81.1
La	58.0		0.5		

Table VI. Cr/Co atomic ratio in the LSC cathode paste after 1000 h at 700°C as calculated from EDX results.

Sample	Cr:Co
LaFeO3	0.29 ± 0.03
LaFeO3 pre-oxidized	<0.01
Cu+LaFeO3	0.56 ± 0.03
Cu+LaFeO3 pre-oxidized	<0.01

pre-oxidized samples in the ASR/Cr retention test. Worth mentioning is that Copper is present in small amounts, mostly in the outer layers.

To evaluate Cr-barrier properties of the perovskite coatings, a detailed EDX analysis was performed in the LSC paste. The result is summarized in Table VI, where the Cr/Co atomic ratio is reported. The $LaFeO_3$ and Cu-$LaFeO_3$ samples are characterized by high values of chromium contamination of the cathode paste, while the pre-oxidized samples show only negligible traces of chromium diffusion in the LSC layer. The absence of chromium in the pre-oxidized samples clearly indicates that the perovskite conversion coatings are very efficient Cr diffusion barriers under IT-SOFC temperature conditions. Since Cr contamination disappears after the pre-oxidation treatment is also a clear indication that some residual salt present on the sample surface after the molten carbonate synthesis is the major Cr contamination source. Although a pre-oxidation treatment was effective in removing Cr residues from the coating surface, strategies for more simple and cost-effective cleanup procedures are currently under investigation.

Conclusions

In this work the effect of a composite dual-phase Cu-$LaFeO_3$ conversion coating on both contact electrical and Cr retention behavior of a K41 18Cr ferritic stainless steel has been evaluated in long-term experiments at 700°C under IT-SOFC oxidizing conditions. By comparison with similar single-phase $LaFeO_3$ perovskite coating samples, the effect of copper on the perovskite conversion coating microstructure and performance has been investigated.

An improved ASR behavior was observed for the Cu-$LaFeO_3$ coatings, although relatively high ASR values in between the 100–200 $m\Omega \cdot cm^2$ range were determined on all the perovskite coating samples. No stable values could be achieved even after 1000 h testing. However, a significant decreasing trend of the ASR values was recorded, suggesting that perovskite conversion coatings are immune to degradation effects, including growth of insulating chromia films. Irregular and rough surface of the perovskite crystals caused a not perfect contact with the LSC cathode paste during the ASR/Cr retention test. This suggests that actual ASR values should be lower than the experimentally determined ones.

An effective cleanup procedure of the coating surfaces after the molten carbonate synthesis step was found to be crucial to eliminate any Cr entrapped in residual salt, which could lead to spurious Cr contamination results. A pre-oxidation treatment in air at 700°C was used as effective cleanup step to remove completely Cr from the coating surfaces, which allowed to demonstrate beyond any doubts that perovskite coatings are effective barriers to Cr migration.

As continuation to our previous study, the present work allowed to examine in more detail the effect of copper on the perovskite conversion coating process. Besides accelerating the perovskite conversion process, this work demonstrates that copper has also a beneficial effect on the conversion coating microstructure promoting the formation of finer $LaFeO_3$ grain sizes and thinner multi-layer structure as compared to similar $LaFeO_3$ coatings that were obtained in copper-free molten carbonate baths. Thus, improved ASR behavior of the dual-phase Cu-$LaFeO_3$ coatings could be explained by changes in the coating microstructure, although some doping effects due to inward copper diffusion through the coating may have also contributed.

Acknowledgments

This work was supported by the European Commission through the FP7 Fuel Cells and Hydrogen Joint Undertaking, grant Agreement 325331 (Steel Coatings for Reducing Degradation in SOFC, SCoReD2.0 Project).

ORCID

S. Frangini https://orcid.org/0000-0002-2080-2129
A. Masi https://orcid.org/0000-0002-1976-0603

References

1. J. Wu and X. Liu, *J. Mater. Sci. Technol.*, **26**, 293 (2010).
2. J. C. W. Mah, A. Muchtar, M. R. Somalu, and M. J. Ghazali, *Int. J. Hydrogen Energy*, **42**, 9219 (2017).
3. Z. Yang, *Int. Mater. Rev.*, **53**, 39 (2008).
4. W. Z. Zhu and S. C. Deevi, *Mater. Sci. Eng. A*, **348**, 227 (2003).
5. Z. Yang et al., *J. Electrochem. Soc.*, **151**, A1825 (2004).
6. N. Shaigan, W. Qu, D. G. Ivey, and W. Chen, *J. Power Sources*, **195**, 1529 (2010).
7. S. Frangini, A. Masci, and F. Zaza, *Corros. Sci.*, **53**, 2539 (2011).
8. S. Frangini, F. Zaza, and A. Masci, *Corros. Sci.*, **62**, 136 (2012).
9. A. Masi, S. Frangini, M. Carlini, A. Masci, and S. J. McPhail, *ECS Trans*, **68**, 1625 (2015).
10. S. Frangini et al., in *Proceedings of the 12th European SOFC & SOE Forum 2016*, p. 24 (2016).
11. A. Masi, S. Frangini, L. Della Seta, S. J. McPhail, and M. Carlini, *J. Electrochem. Soc.*, **164**, F850 (2017).
12. A. Masi et al., *Mater. Corros.*, **68**, 536 (2017).
13. J. Tallgren et al., *ECS Trans.*, **68**, 1597 (2015).
14. J. W. Fergus, K. Wang, and Y. Liu, *ECS Trans.*, **33**, 77 (2011).
15. J. Mizusaki, J. Tabuchi, and T. Matsuura, *J. Electrochem. Soc.*, **136**, 2082 (1989).
16. H. Falk-Windisch, J. Claquesin, M. Sattari, J. -E. Svensson, and J. Froitzheim, *J. Power Sources*, **343**, 1 (2017).
17. S. Licht and H. Wu, *J. Phys. Chem. C*, **115**, 25138 (2011).
18. K. J. Kim, *Chem. Eng. Technol.*, **39**, 1212 (2016).
19. T. Kojima, A. Kojima, T. Miyuki, Y. Okuyama, and T. Sakai, *J. Electrochem. Soc.*, **158**, A1340 (2011).
20. Z. Yang, G. Xia, and J. W. Stevenson, *Electrochem. Solid-State Lett.*, **8**, A168 (2005).
21. X. Montero et al., *J. Electrochem. Soc.*, **156**, B188 (2009).